

Pion Production via Proton Synchrotron Radiation in Strong Magnetic Fields in Relativistic Field Theory: Scaling Relations and Angular Distributions

Tomoyuki Maruyama,^{1,2,3} Myung-Ki Cheoun,^{4,3}

Toshitaka Kajino,^{3,5} and Grant J. Mathews⁶

¹*College of Bioresource Sciences, Nihon University, Fujisawa 252-8510, Japan*

²*Advanced Science Research Center,
Japan Atomic Energy Agency, Tokai 319-1195, Japan*

³*National Astronomical Observatory of Japan,
2-21-1 Osawa, Mitaka, Tokyo 181-8588, Japan*

⁴*Department of Physics, Soongsil University, Seoul, 156-743, Korea*

⁵*Department of Astronomy, Graduate School of Science,
University of Tokyo, Hongo 7-3-1, Bunkyo-ku, Tokyo 113-0033, Japan*

⁶*Center of Astrophysics, Department of Physics,
University of Notre Dame, Notre Dame, IN 46556, USA*

(Dated: April 5, 2024)

Abstract

We study pion production by proton synchrotron radiation in the presence of a strong magnetic field when the Landau numbers of the initial and final protons are $n_{i,f} \sim 10^4 - 10^5$. We find in our relativistic field theory calculations that the pion decay width depends only on the field strength parameter which previously was only conjectured based upon semi-classical arguments. Moreover, we also find new results that the decay width satisfies a robust scaling relation, and that the polar angular distribution of emitted pion momenta is very narrow and can be easily obtained. This scaling implies that one can infer the decay width in more realistic magnetic fields of 10^{15}G , where $n_{i,f} \sim 10^{12} - 10^{13}$, from the results for $n_{i,f} \sim 10^4 - 10^5$. The resultant pion intensity and angular distributions for realistic magnetic field strengths are presented and their physical implications discussed.

PACS numbers: 95.85.Ry, 24.10.Jv, 97.60.Jd,

It is widely accepted that soft gamma repeaters (SGRs) and anomalous X-ray pulsars (AXPs) correspond to magnetars [1], and that the associated strong magnetic fields may have a significant role in the production of high energy photons. Furthermore, short duration gamma-ray bursts (GRBs) may arise from highly magnetized neutron stars [2] or mergers of binary neutron stars [3–5], and the most popular theoretical models for long-duration GRBs invoke [6–9] a magnetized accretion disk around neutron stars or rotating black holes (collapsars) for their central engines. Such magnetars (or black holes with strong magnetic fields) have also been proposed [10, 11] as an acceleration site for ultra high-energy (UHE) cosmic rays (UHECRs) and a possible association [12] between magnetic flares and UHECRs has also been observed.

In this letter we consider the synchrotron emission that can be produced by high-energy protons accelerated in such environments containing a strong magnetic field. This process has been proposed as a source for high-energy photons in the GeV – TeV range [13–18], possibly in association with GRBs. Of interest to the present work is the fact that meson-nucleon coupling is about 100 times larger than the photon-nucleon coupling, and the meson production process is expected to exceed photon synchrotron emission in the high energy regime. For example, Refs. [19–23] addressed the possibility of π^0 emission from protons in a strong magnetic field. The subsequent decay of such π^0 s may be an additional source of the observed TeV gamma rays in association with supernova remnants [24].

However, previous calculations were performed in a semi-classical approximation to the exact relativistic quantum-mechanical treatment of the proton transitions among the Landau levels of the strong magnetic field. Also, there is ambiguity in the literature as to the proper behavior of production in the strong field limit (cf. [20]). In this letter we resolve this ambiguity in an exact (Quantum Field Theory) QFT calculation.

In our previous work [25] we exploited the Green’s function method for the propagation of protons in a strong magnetic field, and studied the pion production from proton synchrotron emission in a relativistic quantum approach, whereby the pion is produced from the transition of a proton between two Landau levels.

We then deduced the energy and angular distribution of emitted pions which had not been deduced in previous semi-classical approaches. Furthermore, we found that the anomalous magnetic moment (AMM) of the proton enhances the emission decay width by about a factor of 50. This huge effect comes from the fact that the overlap integral of the two harmonic

oscillator (HO) wave functions is significantly altered by a small shift owing to the AMM of the HO quantum numbers in the pion production energy region [25].

In that previous work, however, it was untractable to numerically evaluate Landau numbers greater than ~ 300 . Therefore, we calculated the emission rate for a magnetic field strength of $B \approx 5 \times 10^{18} \text{G}$ for which fewer Landau levels were required.

In the present work we develop a new method and a new scaling relation to give results for a much larger number of the Landau levels and for realistic magnetic field strengths.

In the semi-classical approach for the production of synchrotron radiation, the magnetic field strength is characterized by the curvature parameter, $\chi = e_i^3/(m^3 R_c)$ given in terms of the incident particle mass m , its energy e_i , and the curvature radius R_c . For protons propagating in a strong magnetic field, the value of χ can be written as

$$\chi = \frac{e_i^2}{m_p^3 R_c} = \frac{e B e_i}{m_p^3}, \quad (1)$$

where m_p is the proton mass. Pion production is the dominant process compared to direct photon emission when $\chi \sim 0.01 - 1$ [19].

There are various semi-classical calculations [19–23] which give different results, but all of those models suggest that the decay width depends only on the parameter χ , not on the initial energy e_i and the strength of the magnetic field B individually, though this has not been confirmed.

In this work, therefore, we have developed a new numerical method, so that we can examine the scaling relation for magnetic field strengths $\sim 10^{17} - 10^{18} \text{G}$, that are weaker than on our work [25]. Though this strength is still large, we also find a new robust scaling rule in the quantum calculation. Based upon this we can realistically estimate for the first time the results for a much larger number of Landau numbers, i.e. lower magnetic field than previous calculations, from the results obtained from a smaller number of Landau levels.

Here, we briefly explain our approach.

We assume a uniform magnetic field along the z -direction, $\mathbf{B} = (0, 0, B)$, and take the electro-magnetic vector potential A^μ to be $A = (0, 0, xB, 0)$ at the position $\mathbf{r} \equiv (x, y, z)$.

The relativistic proton wave function $\tilde{\psi}$ is obtained from the following Dirac equation:

$$\left[\gamma_\mu \cdot (i\partial^\mu - eA^\mu) - m_p - \frac{e\kappa_p}{2m_p} \sigma_{\mu\nu} (\partial^\mu A^\nu - \partial^\nu A^\mu) \right] \tilde{\psi}(x) = 0, \quad (2)$$

where κ_p is the proton AMM and e is the elementary charge. Here, we scale all variables with \sqrt{eB} as $X_\mu = \sqrt{eB}x_\mu$ and $M_p = m_p/\sqrt{eB}$. The proton single particle energy is then

written as

$$E(n, P_z, s) = \sqrt{P_z^2 + (\sqrt{2n + M_p^2} - s\kappa_p/M_p)^2}. \quad (3)$$

When we use the pseudo-vector coupling for the πN -interaction, we can obtain the differential decay width of the proton as

$$\frac{d^3\Gamma_{p\pi}/\sqrt{eB}}{dQ^3} = \frac{1}{8\pi^2 E_\pi} \left(\frac{f_\pi}{M_\pi} \right)^2 \sum_{n_f, s_f} \frac{\delta(E_f + E_\pi - E_i)}{4E_i E_f} W_{if}, \quad (4)$$

with

$$W_{if} = \text{Tr} \left\{ \rho_M(n_i, s_i, P_z) \mathcal{O}_\pi \rho_M(n_f, s_f, P_z - Q_z) \mathcal{O}_\pi^\dagger \right\}, \quad (5)$$

where f_π is the pseudo-vector pion-nucleon coupling constant, $M_\pi = m_\pi/\sqrt{eB}$ with m_π being the pion mass, and

$$\begin{aligned} \rho_M = & \left[E\gamma_0 + \sqrt{2n}\gamma^2 - P_z\gamma^3 + M_p + (\kappa_p/M_p)\Sigma_z \right] \\ & \times \left[1 + \frac{s}{\sqrt{2n + M_p^2}} (\kappa_p/M_p + P_z\gamma_5\gamma_0 - E\gamma_5\gamma^3) \right], \end{aligned} \quad (6)$$

$$\begin{aligned} \mathcal{O}_\pi = \gamma_5 \left\{ \left[\mathcal{M}(n_i, n_f) \frac{1 + \Sigma_z}{2} + \mathcal{M}(n_i - 1, n_f - 1) \frac{1 - \Sigma_z}{2} \right] [\gamma_0 Q_0 - \gamma^3 Q_z] \right. \\ \left. - \left[\mathcal{M}(n_i, n_f - 1) \frac{1 + \Sigma_z}{2} + \mathcal{M}(n_i - 1, n_f) \frac{1 - \Sigma_z}{2} \right] \gamma^2 Q_T \right\}. \end{aligned} \quad (7)$$

In the above equation, the pion momentum scaled by \sqrt{eB} is written as $Q \equiv q/\sqrt{eB} = (E_\pi, 0, Q_T, Q_z)$, and the HO overlap function $\mathcal{M}(n_1, n_2)$ is defined [25] as

$$\mathcal{M}(n_1, n_2) = \int dx f_{n_1} \left(x - \frac{Q_T}{2} \right) f_{n_2} \left(x + \frac{Q_T}{2} \right). \quad (8)$$

For these conditions the system is translationally symmetric, and quantities with a finite p_{iz} are given by a Lorentz transformation along the z -direction. For example, the decay width can be written as $\Gamma_{p\pi}(p_z) = \Gamma_{p\pi}(p_z = 0) \sqrt{1 - (p_z/e_i)^2}$. Then, we restrict the calculations to $p_{iz} = 0$ at first.

In the realistic condition, $B \sim 10^{15}\text{G}$ and $\chi = 0.01 - 1$, the initial Landau number becomes $n_i \sim 10^{12} - 10^{14}$, and it is almost impossible to calculate $\mathcal{M}(n_i, n_f)$ directly. In the following, we introduce an approximate, but very efficient, method for alleviating this difficulty.

In Fig. 1 we present the decay widths as a function of $(n_i - n_f)/n_i$ when the parameter χ is fixed. The upper panels show the results with the AMM included for $\chi = 0.02$ (a)

and $\chi = 0.07$ (b), and the lower panels show the results without the AMM for $\chi = 0.02$ (c) and $\chi = 0.07$ (d). The dashed, dot-dashed, solid and dotted lines show the results with initial Landau numbers, $n_i = 5 \times 10^3$, 2×10^4 , 6×10^4 and 10^5 , respectively. In all results the initial and final proton spins are set to be $s_i = -s_f = -1$ because this is the dominant contribution.

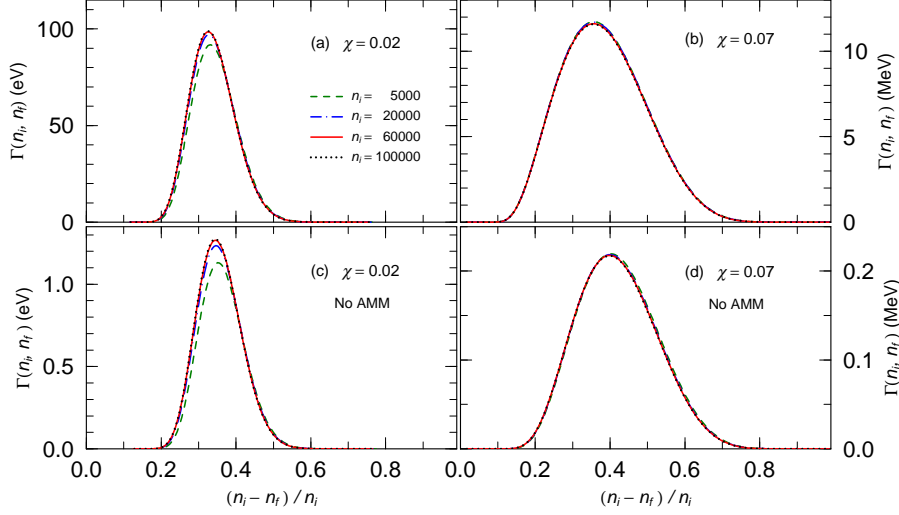


FIG. 1. (Color online) Pion decay widths of protons when $s_i = -s_f = -1$ as a function of $(n_i - n_f)/n_i$ for $\chi = 0.02$ (a) and $\chi = 0.07$ (b). The bottom panels (c) and (d) show the results without the AMM for $\chi = 0.02$ and $\chi = 0.07$, respectively. The dashed, dotted-dashed solid and dotted lines represent the results with initial Landau number, $n_i = 5 \times 10^3$, 2×10^4 , 6×10^4 and 10^5 , respectively.

First, we note that the dependence of the decay width on $\Delta n_{if}/n_i = (n_i - n_f)/n_i$ for the different cases is almost completely identical. That is, they nearly overlap when χ is fixed. In particular, the difference between $n_i = 6 \times 10^4$ and $n_i = 10^5$ is not discernible. There are however various semi-classical calculations [19–23] which give different results, but all of the models indicate that the decay width depends only on the parameter χ , not on the initial energy e_i and the magnetic field B . Thus, we confirm that this scaling relation is satisfied in the quantum calculations, particularly for $n_i \gtrsim 6 \times 10^4$, independently of the AMM.

In the all results the peak positions are at $\Delta n_{if}/n_i \approx 0.3 - 0.4$. As χ increases, the peak position is only slightly shifted to a larger value, and the peak width becomes slightly broader.

When comparing the results with the AMM included (a,b) and those without the AMM

(c,d), we see that the AMM still increases the decay widths significantly even in the present conditions where magnetic fields are much weaker and the initial Landau numbers are much larger than those in the previous work, $B = 5 \times 10^{18} \text{G}$ and $n_i \approx 48$. [25].

Moreover, we see that the peak position is shifted by including the AMM with the scaling relation being satisfied. This result indicates that the AMM remains important for any magnetic field strength and proton energy.

As written in Ref. [25], the very large effect of the AMM comes from the shift of this peak position, i.e. where the HO overlap integral $\mathcal{M}(n_i, n_f)$ changes rapidly. For $n_i \approx 48$ and a shift of Δn_{if} to 2, the absolute value of \mathcal{M} increases by about a factor of 100. When the magnetic field is weaker or the initial energy becomes larger, n_i increases, and the AMM effect is expected to be smaller. When χ is fixed, however, the AMM effect remains and plays an important role in any regime.

Furthermore, from Fig. 1, we note that the Landau level difference in the pion emission between the initial and final states is of the same order as that of the initial and final Landau numbers, $\Delta n_{if} \sim n_i \sim n_f$.

In the adiabatic limit it can be assumed that the relative momentum between the final proton and the pion is zero, and that the two particles have nearly the same velocity. In that limit the ratio between these two energies is the same as the mass ratio: $e_\pi/e_f \approx m_\pi/m_p$, and the final proton and pion energies become

$$e_f \approx \frac{m_p}{m_p + m_\pi} e_i, \quad e_\pi \approx \frac{m_\pi}{m_p + m_\pi} e_i. \quad (9)$$

If the initial proton energy is very large $e_i \gg m_p$, $E_{i,f} \approx \sqrt{2n_{i,f}}$, so that in the adiabatic and high energy limit the following relation holds: $\sqrt{n_i} - \sqrt{n_f} \approx (m_\pi/m_p)\sqrt{n_i}$. This leads to

$$\Delta n_{if} \equiv n_i - n_f \approx \frac{m_p^2 - (m_p - m_\pi)^2}{m_p^2} n_i \approx 0.28 n_i. \quad (10)$$

The actual πN -interaction is via a p -wave, and the relative momentum is not zero even in the adiabatic limit. Thus, the actual value of Δn_{if} in Fig. 1 is larger than the above value; this argument is consistent with the present results.

In Fig. 2, we show contour plots of the luminosity distribution of the emitted pions, $d^3 I/dq^3 = e_\pi d^3 \Gamma_{p\pi}/dq^3$, where the initial proton is at $p_{iz} = 0$ and $n_i = 5 \times 10^3$ (a), 2×10^4 (b), or 6×10^4 (c) with $\chi = 0.04$. The pion momentum is distributed narrowly in the z -direction

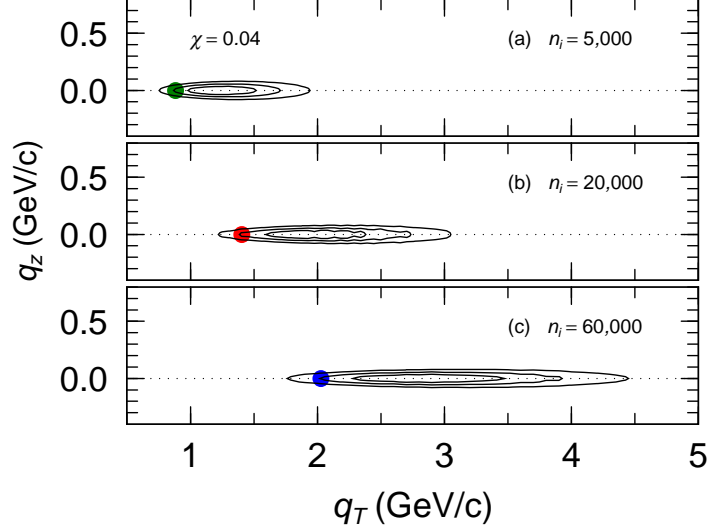


FIG. 2. (Color online) Contour plot of the differential pion luminosity for the initial spin state $s_i = -1$ and $\chi = 0.04$ at $p_{iz} = 0$ with initial Landau numbers, (a) $n_i = 5 \times 10^3$, (b) 2×10^4 and (c) 6×10^4 . Lines on each plot show the relative strength, 25%, 50% and 75%. The vertical and horizontal axes are the z -component and the transverse component of the emitted pion momentum. The large dots show the adiabatic limit.

independently of n_i , but is broadly distributed in the transverse direction. The width in the z -direction is almost independent of n_i , but the width in the transverse direction becomes larger as the initial Landau number n_i increases. It means that most pions are emitted in the transverse direction when $p_{iz} = 0$ in the limit of $n_i \rightarrow \infty$.

When $n_{i,f}$ and $s_{i,f}$ are fixed, the differential decay width is proportional to the HO overlap integral $\mathcal{M}(n_i, n_f)$ in Eq. (8), which is an oscillating function with respect to Q_T^2 , $\mathcal{M}(n_1, n_2) = \mathcal{M}(n_1, n_2, Q_T^2)$, but the actual value of Q_T^2 in the present calculations turns out to be restricted to the region below the first peak. When $Q_T^2 \ll 1$, $\mathcal{M}(n_1, n_2, Q_T^2) \propto Q_T^{n_1 - n_2}$, and thus \mathcal{M} is a monotonic and very rapidly increasing function in the region for our calculations. So, the decay width has an effective strength only around the maximum value of Q_T^2 . This effective region becomes narrower as $\Delta n_{i,f}$ increases.

The momentum region of the emitted pions when $p_{iz} \neq 0$ can then be calculated from the results with $p_{iz} = 0$ by a Lorentz transformation along the z -direction. Since the pion is emitted in the transverse direction when $p_{iz} = 0$, the z -component of the velocity for the emitted pion and the final proton are equal to that of the initial proton, namely

$P_{iz}/E_i = P_{fz}/E_f = Q_z/E_\pi$, which leads to $Q_z/Q_T \approx P_{iz}/\sqrt{2n_i} \approx P_{iz}/\sqrt{2n_f}$. Hence, when $p_{iz} \neq 0$, the differential decay width is given by

$$\frac{d^3\Gamma_{p\pi}(n_i, s_i)}{dq^3} = \frac{\sqrt{e_\pi^2 - q_z^2}}{2\pi e_\pi^2} \sum_{n_f} \Gamma(n_i, s_i, n_f, -s_i) \delta(e_\pi - e_i + e_f) \delta\left(q_z - \frac{e_\pi}{e_i} p_{iz}\right). \quad (11)$$

When the magnetic field is taken to be $B \sim 10^{15}\text{G}$, the initial energy of the proton should be a several TeV, and the Landau number of the initial state should be order of $10^{12} - 10^{13}$. Performing a quantum calculation is not realistic in such a condition. However, we can calculate $\Gamma(n_i, n_f)$ with $n_i \sim 10^4$ and extrapolate it to $n_i \sim 10^{12}$ via the above scaling relation. In this way we can calculate the decay width in any realistic conditions.

Hereafter, we apply the scaling relation to the case of a realistic strength of the magnetic field $B \sim 10^{15}\text{G}$ by using the above equation (11).

In Fig. 3 we show the pion decay widths for protons with $p_{iz} = 0$ and $s_i = -1$ as functions of the initial energy when $B = 10^{15}\text{G}$. The solid and dot-dashed lines represent the decay widths of the proton with and without the AMM, respectively. For comparison, we also give the results in the semi-classical approaches of Ref. [19] with the dashed line.

In the quantum approach we calculate the decay width with $n_i = 160,000 - 1,000,000$ and extrapolate them to that when $n_i \sim 10^{12}$, by using the scaling relation.

First, we can confirm that the AMM still increases the decay widths significantly even in the realistic conditions where the magnetic fields are much weaker and the initial Landau numbers are much larger than those in the previous work, $B = 5 \times 10^{18}\text{G}$ and $n_i \approx 48$. [25].

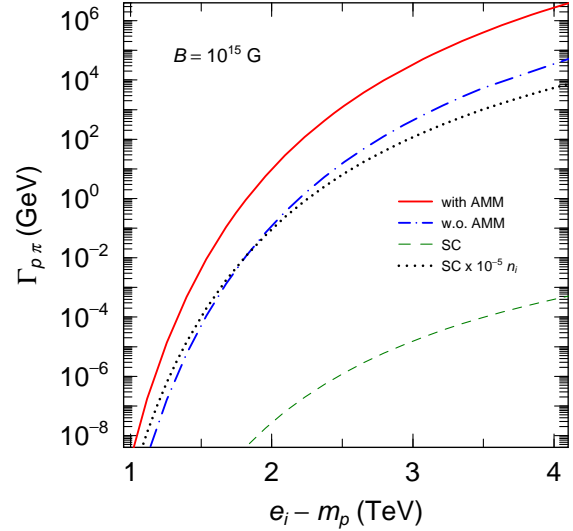


FIG. 3. (Color online) Decay width of a proton with $p_{iz} = 0$ and $s_i = -1$ due to synchrotron emission as a function of the proton initial energy $e_i - m_p$ when $B = 10^{15}\text{G}$. The solid and dot-dashed lines represent the decay widths with and without the AMM, respectively. The dashed and dotted lines indicate the results in the semi-classical calculations [19] and those multiplied with $10^{-5}n_i$, respectively

Second, we see that the quantum results are much larger than those in the semi-classical approach. As mentioned before, one assumes that $\Delta n_{if} \ll n_i$ in that approach and that the phase-space of the final pion is very small. In Ref. [19] they assumed that the pion energy is the same as the pion mass $e_\pi = m_\pi$, so that the total decay width does not depend on the initial energy if χ is fixed.

In the quantum calculation, on the other hand, the energy of the emitted pion is of the same order as the initial proton energy, and the scaling relation about $\Gamma(n_i, n_f)$ shows that the total decay width is proportional to the initial Landau number, $\Gamma_{p\pi}(n_i) \propto n_i$.

In order to examine this, we multiply by a factor proportional to the initial Landau number, $10^{-5}n_i$, with the decay width in the semi-classical calculation and show this result with the dotted line. This result is qualitatively similar to that without the AMM in the quantum approach; we should note that if we use the factor, $10^{-3}n_i$, the result is close to that with the AMM. It can be conjectured from this result that the main difference in the total decay width between the quantum approach and the semi-classical approach comes from the naive estimate of the energy of the emitted pions and their phase space volume.

Next, we study the photon luminosity distribution, d^3I_γ/dq_γ^3 at $q_{\gamma z} = 0$, for a realistic magnetic field strength of $B = 10^{15}\text{G}$, where q_γ is the momentum of the emitted photon which is a half of the emitted pion momentum, $q_\gamma = q/2$, in the ultra-relativistic limit.

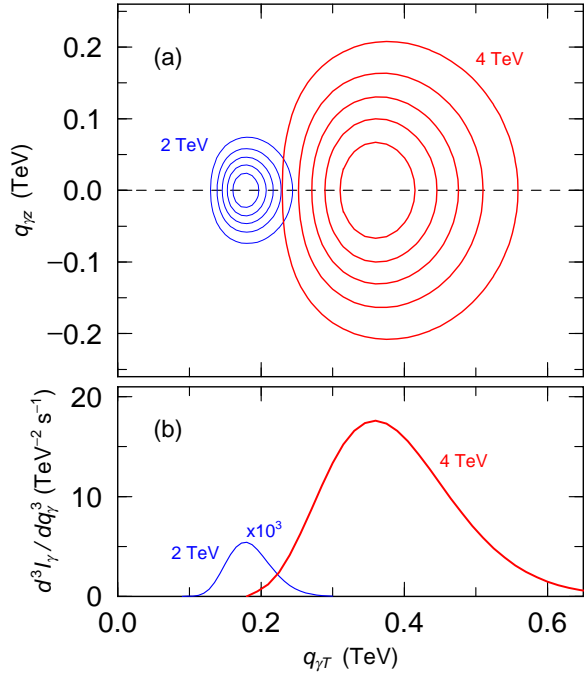


FIG. 4. (Color online) The differential luminosities per a proton versus the photon momentum. They are integrated over the initial proton angle. Upper panel shows contour plots at an initial proton energy $e_i - m_p = 2 \text{ TeV}$ (thin line) and 4 TeV (thick line). Lower panel shows the luminosity distribution at $q_z = 0$ when $e_i - m_p = 2 \text{ TeV}$ and $e_i - m_p = 4 \text{ TeV}$. The former result is reduced by a factor of 10^4 .

We assume that the momentum distribution of the initial proton is spherical and make an average of the luminosity over the proton angles. In Fig. 4 we show the luminosity distribution per a proton when the initial proton energies are $e_i - m_p = 2$ and 4 TeV, and the magnetic field $B = 10^{15}$ G; this is a more realistic representation of the magnetar environment.

In the upper panel (a) the (blue) thin and (red) thick lines show contour plots for $e_i - 2m_p = 2$ TeV and 4 TeV, respectively. In the lower panel (b) we show the distribution d^3I_γ/dq^3 at $q_z = 0$ for $e_i - m_p = 2$ TeV and 4 TeV.

As noted above, the incident proton emits a pion, whose energy is $\sim 10-30$ % (depending upon χ) of the incident proton energy, along the same direction as that of the incident proton momentum. This emitted pion decays into two photons with the same energy and the same direction of their movement in this ultra-relativistic energy region.

The proton transverse momentum is proportional to $\sqrt{\chi}$, and the decay width rapidly decreases as χ become smaller. Then, the luminosities mainly distribute in a region perpendicular to the magnetic field, though they also distribute about 40 - 60 % of the photon momentum along the direction of the magnetic field.

In summary, we have calculated the exact pion decay width of protons in the relativistic quantum approach including the Landau levels and the AMM for a magnetic field strength in the range $B = 10^{18} - 10^{17}$ G, where the maximum Landau levels are $n_{max} \approx 5 \times 10^3 - 10^5$. As the magnetic field becomes weaker, and the Landau number tremendously increases, the polar angular distributions of the emitted pion momentum becomes narrower, when the initial and final proton Landau numbers are fixed. Then, the polar angles of the emitted pion and the final proton momenta are almost the same as that of the initial proton.

The large effect of the AMM and the very narrow width of the polar angular distribution are caused by a rapid change of the HO overlap integral $\mathcal{M}(n_i, n_f)$.

As the energy of incident proton increases or the magnetic field is weaker, the distribution of emitted pion momentum $|\mathbf{q}|$ on the $q_z - q_T$ plane is elongated in the radial direction, keeping the width along q_z narrow, because the dominant transition between the two Landau levels is as large as $\Delta n_{if}/n_i \gtrsim 0.3$ in $\Gamma(n_i, n_f)$. As such, the quantity $\Gamma(n_i, n_f)$ depends only on $\Delta n_{if}/n_i$ and $\chi = eBe_i/m_p^3$.

In the usual semi-classical approximations it is assumed that $\Delta n_{if} \equiv n_i - n_f \ll n_i$, where the HO overlap integral \mathcal{M} can be approximated with an Airy function. This assumption is

equivalent to the adiabatic limit when the produced particle is massless such as a photon.

Furthermore, the very low energy of emitted particles leads to a small phase space volume in the final particle momentum space and causes the total decay width to be underestimated. This underestimation becomes larger as the initial proton energy increases. As the mass of the produced particle becomes larger, its emitted momentum increases. Thus, our calculation suggests a change in the semi-classical relation between the production rate and χ .

In conclusion, the present work suggests a better way to treat pion production. Although direct calculation with a realistic magnetic field and a large number of Landau levels is not tractable, the result that $\Gamma(n_i, n_f)$ depends only on χ and $\Delta n_{if}/n_i$ demonstrates that one can calculate $\Gamma(n_i, n_f)$ for values of $n_i \sim 10^{4-5}$ and scale those results to more realistic conditions. Also, when $p_{iz} \neq 0$, the decay width can be obtained from a Lorentz transformation along the z -direction.

By using this scaling relation we can, for the first time, present the luminosity distribution of photons due to the pion production process in realistic environments where the magnetic field is $B = 10^{15}\text{G}$ and the incident proton energy is $e_i - m_p = 2$ and 4 TeV.

In this work, we have found the energy distribution of emitted particles and the large effect of the AMM in the particle production from the synchrotron radiation. These features turn out to be caused by properties of the HO overlap function, $\mathcal{M}(n_i, n_f)$, which is written in terms of the associated Laguerre function, $L_{n_f}^{n_i - n_f}(Q_T^2/2)$ [25]. We do not know its asymptotic form when $n_i \sim n_f \rightarrow \infty$, and we cannot prove the above features analytically at present, although we deduce an efficient scaling relation in the function. If we knew it, we could make a general formulation for all kinds of particle production. This we leave to a future work.

In other future works, we will be able to calculate the emitted photon distribution and the magnetic structure of magnetars using our method and obtain significant information from observations of energetic photons from magnetars.

This work was supported in part by Grants-in-Aid for Scientific Research of JSPS (26105517, 24340060) of the Ministry of Education, Culture, Sports, Science and Technology of Japan, and also by the National Research Foundation of Korea (Grants No. NRF-2014R1A2A2A05003548). Work at the University of Notre Dame is supported by the

- [1] S. Mereghetti, *Annu. Rev. Astron. Astrophys.*, **15**, 225 (2008).
- [2] A.M. Soderberg , S.R. Kulkarni, E. Nakar et al., *Natur*, **442**, 1014 (2006).
- [3] N. Gehrels, C.L. Sarazin, P.T. O’Brien et al., *Natur*, **437**, 851 (2005).
- [4] J.S. Bloom, J.X. Prochaska and D. Pooley et al., *ApJ*, **638**, 354 (2006).
- [5] N.R. Tanvit, A.J. Levan, A.S. Fruchter et al., *Natur*, **500**, 547 (2013).
- [6] A.I. MacFadyen, S.E. Woosley, *ApJ*, **524**, 262 (1999).
- [7] A.I. MacFadyen, S.E. Woosley, A. Heger, *ApJ*, **550**, 890 (2001).
- [8] S. Harikae, T. Takiwaki and J. otake, *ApJ*, **704**, 354 (2009).
- [9] S. Harikae, K. Kotake, T. Takiwaki and Y.-i Sekiguchi, *ApJ*, **720**, 614 (2010).
- [10] M.A. Hillas, *Annu. Rev. Astron. Astrophys.*, **22**, 425 (1984).
- [11] J. Aarons, *ApJ*, **589**, 871 (2003).
- [12] K. Ioka, S. Razzaque, S. Kobayashi and P. Mészáros, *ApJ*, **633**, 1013 (2005).
- [13] N. Gupta and B. Zhang, *MNRAS*, **380**, 78 (2007).
- [14] M. Böttcher, C. D. Dermer, *ApJL*, **499**, L131 (1998).
- [15] T. Totani, *ApJL*, **502**, L13 (1998).
- [16] P.C. Fragile, G.J. Mathews, J. Poirier and T. Totani, *APh* **20**, 591 (2004).
- [17] K. Asano and S. Inoue, *ApJ*, **671**, 645 (2007) .
- [18] K. Asano, S. Inoue and P. Mészáros, *ApJ*, **699**, 953 (2009).
- [19] A. Tokushita and T. Kajino, *ApJ*, **525**, L117 (1999).
- [20] V. Berezhinsky, A. Dolgoy and M. Kachelriess, *Phys. Lett. B* **351**, 261 (1995)
- [21] V.L. Ginzburg and S.I. Syrovatskii, *UsFiN*, **87**, 65 (1965).
- [22] V.L. Ginzburg and S.I. Syrovatskii, *Annu. Rev. Astron. Astrophys.* **3**, 297 (1965).
- [23] G.F. Zharkov, *Sov. J. Nucl. Phys.*, **1**, 17314 (1965).
- [24] A.A. Abdo et al., *Science*, **327**, 1103 (2010).
- [25] T. Maruyama, M.-K. Cheoun, T. Kajino, Y. Kwon, G.J. Mathews, C.Y. Ryu, *Phys. Rev. D* **91**, 123007 (2015).